Available online at www.sciencedirect.com

SciVerse ScienceDirect

Journal of Nutritional Biochemistry 23 (2012) 1302–1313

Journal of Nutritional Biochemistry

Consumption of high-fat diet induces tumor progression and epithelial–mesenchymal transition of colorectal cancer in a mouse xenograft model

Feng-Yao Tang[a,*], Man-Hui Pai[b], En-Pei Isabel Chiang[c]

[a]Department of Nutrition, Biomedical Science Laboratory, China Medical University, Taichung 40402, Taiwan
[b]Department of Anatomy, Taipei Medical University, 11031 Taipei, Taiwan
[c]Department of Food Science and Biotechnology, National Chung-Hsing University, 404 Taichung, Taiwan

Received 24 December 2010; received in revised form 9 June 2011; accepted 27 July 2011

Abstract

Epidemiologic studies suggest that intake of high-fat diet (HFD) promotes colon carcinogenesis. Epithelial–mesenchymal transition (EMT) and inflammation play important roles during tumor progression of colorectal cancer (CRC). Oncogenic pathways such as phosphatidylinositol-3-kinase (PI3K)/Akt/mTOR and mitogen-activated protein kinase (MAPK)/ERK signaling cascades induce EMT and inflammation in cancer. No experimental evidence has been demonstrated regarding HFD-mediated tumor progression including EMT in CRC so far. Our results demonstrated that HFD consumption could induce tumor growth and progression, including EMT and inflammation, in a mouse xenograft tumor model. The molecular mechanisms were through activation of MAPK/ERK and PI3K/Akt/mTOR signaling pathways. HFD induced up-regulation of cyclooxygenase-2, cyclin D1 and proliferating cell nuclear antigen proteins concomitant with increases in expression of nuclear factor-κB p65 (RelA) and β-catenin proteins. Surprisingly, HFD consumption could suppress $p21^{CIP1/WAF1}$ expression through increases in nuclear histone deacetylase complex (HDAC). Moreover, HFD could mediate the disassembly of E-cadherin adherent complex and the up-regulation of Vimentin and N-cadherin proteins in tumor tissues. Taken together, our novel findings support evidence for HFD-mediated modulation of HDAC activity and activation of oncogenic cascades, which involve EMT and inflammation in CRC, playing important roles in tumor growth and progression in a mouse xenograft model.

Keywords: High-fat diet; Histone deacetylase; Cyclooxygenase-2; Epithelial–mesenchymal transition; Colorectal cancer

1. Introduction

Colorectal cancer (CRC) is one of the leading causes of malignancy-related death in many countries. In the United States alone, nearly 50,000 deaths are attributed to this cancer annually [1]. Epidemiologic studies reported a significant association between Western-style diet (characterized by high intake of dietary fat) and increased recurrence or mortality in patients with CRC [2–4]. Colon carcinogenesis is featured with aberrant regulation of tumor growth and progression, including epithelial–mesenchymal transition (EMT) and tumor inflammation [5–7]. Acquisition of multiple tumor-associated mutations including aberrant activation of epidermal growth factor receptor could lead to the genomic instability [8]. Oncogenic pathways such as phosphatidylinositol-3-kinase (PI3K)/Akt/mTOR and mitogen-activated protein kinase (MAPK)/ERK signaling cascades play important roles in the development of CRC [9,10]. It is well known that downstream target molecules of PI3K including Akt and mTOR proteins regulate cell cycle progression and growth of cancer cells [11,12]. Under the further activation of PI3K/Akt signaling pathway, the nuclear factor-κB (NF-κB) inhibitor protein (IκBα) is phosphorylated by IκBα kinase and is subjected to ubiquitin-mediated degradation [13]. Degradation of IκBα allows the nuclear translocation of activated NF-κB p65 (RelA) proteins and the up-regulation of cyclooxygenase-2 (COX-2) gene in cancer cells. Over-expression of COX-2 is frequently observed in the inflammation and progression of colorectal tumors [7,14,15].

Mutations of KRAS/BRAF oncogenes could further drive the MAPK/ERK signaling cascade and get involved in accelerated cell cycle progression and proliferation of cancer cells [16]. During the proliferation of colon cancer cells, cell-cycle-related proteins such as cyclin D1 and proliferating cell nuclear antigen (PCNA) are major regulators for cell cycle progression and DNA replication, respectively [17,18]. Aberration activation of PI3K/Akt/mTOR and MAPK/ERK signaling cascades could induce tumor growth and progression through increases in β-catenin, Vimentin and cyclin D1 expression [19–21]. Functions of cyclin D1 and PCNA proteins are suppressed by cell cycle inhibitor $p21^{CIP1/WAF1}$ protein [22,23]. A recent study indicated that histone deacetylase complex (HDAC) is involved in the deacetylation of promoter region in chromosome and suppression of tumor suppressor genes such as $p21^{CIP1/WAF1}$ [24,25]. Therefore, expression of $p21^{CIP1/WAF1}$ is inversely correlated with HDAC activity [26]. These findings suggest that functional loss of tumor suppressor

* Corresponding author. Tel.: +886 4 22060643; fax: +886 4 22062891.
E-mail address: vincenttang@mail.cmu.edu.tw (F.-Y. Tang).

0955-2863/$ - see front matter © 2012 Elsevier Inc. All rights reserved.
doi:10.1016/j.jnutbio.2011.07.011

genes and oncogenic mutation of multiple signaling cascades are associated with tumor growth and progression of CRC [10].

EMT is a crucial mechanism regulating the initial steps in tumor metastasis [7,27]. EMT provides cells the ability to migrate and invade, and reflects the plasticity of epithelial cells [28]. While epithelial cells undergo EMT, they acquire a mesenchymal phenotype, including decreased cell–cell adherent junctions and increased motility and chemotherapeutic resistance [28]. It has been reported that EMT is involved in the progression of carcinomas of different sites including colon, head and neck, pancreas, liver, esophagus and lung [29–37]. E-cadherin adherent complexes are major constituents of epithelial junction systems in normal colorectal epithelium [38]. Loss of E-cadherin proteins and augmented expression of Twist, Vimentin and N-cadherin proteins are considered as key steps in EMT [20,21,39–42]. A recent study indicates that overexpression of COX-2 under the regulation of PI3K/Akt/NF-κB pathway is associated with EMT in several types of human cancer [43]. Previous studies showed that activation of MAPK/ERK signaling pathway up-regulated transcriptional factors such as Snail and Slug proteins and suppressed the expression of E-cadherin adhesion molecule [21,44–48]. In contrast, suppression of ERK1/2 and PI3K/Akt/NF-κB signaling cascades could induce the mesenchymal-to-epithelial reverting transition with increasing E-cadherin expression in cancer cells [46,49]. These results suggested that oncogenic activation of signaling pathways such as MAPK/ERK and PI3K/Akt/NF-κB signaling molecules and COX-2 expression play important roles in the development of EMT in CRC.

Many epidemiologic studies demonstrated that high-fat diet (HFD) consumption is correlated with a high prevalence of colon cancer [4]. The activation of inflammation pathway is likely correlated with HFD consumption [50]. These findings suggest that HFD could mediate the development of EMT and tumor inflammation through up-regulation of COX-2 and activation of multiple signaling cascades including PI3K/Akt/NF-κB cascades. However, to date, the *in vivo* effects of HFD consumption on tumor growth and progression including EMT and tumor inflammation in CRC have not been demonstrated yet. The current study was undertaken to evaluate whether HFD (45% of total energy intake) could modulate the tumor progression as well as the correlation between EMT and tumor inflammation in a mouse xenograft tumor model.

2. Materials and methods

2.1. Reagents and antibodies

Anti-phosphorylation ERK1/2, anti-PCNA, anti-cyclin D1, anti-β-catenin, anti-NF-κB p65 (RelA), anti-$p21^{CIP1/WAF1}$, anti-E-cadherin, anti-N-cadherin, anti-Twist, anti-COX-2, anti-lamin A/C and anti-phosphorylation mTOR antibodies were purchased from Cell Signaling Technology, Inc. (Danvers, MA, USA). Anti-β-actin antibody was purchased from Sigma (St. Louis, MO, USA). Anti-Vimentin antibody was purchased from Santa-Cruz Biotechnology, Inc. (Santa Cruz, CA, USA). McCoy's medium and phosphate-buffered saline were purchased from Invitrogen, Inc. (Carlsbad, CA, USA).

2.2. Cell culture

Briefly, HT-29 colon cancer cells were cultured in a 37°C humidified incubator with 5% CO_2 and grown to confluency using fetal bovine serum (FBS)-supplemented McCoy's media. Cells used in different experiments have similar passage number. McCoy's medium was supplemented with 10% heat-inactivated FBS, 2 mM L-glutamine and 2 g/L sodium bicarbonate in the absence of antibiotics.

Table 1
Composition of experimental diets

	SD	HFD
Lipids	13.50	45.70
SFA	3.05	17.52
MUFA	3.31	18.05
PUFA	7.14	10.12
Proteins	27.50	18.30
Carbohydrates	59.00	36.00
Fat/carbohydrate ratio	0.23	1.26

Values are in percent of total energy provided.

Table 2
Consumption of HFD significantly increased the weight of visceral fat pad, tumor tissues and total body weight

	Tumor weight (g)	Weight of visceral fat pad (g)	Total body weight (g)
SD_T (n=9)	0.15±0.03	0.31±0.05	19.52±0.76
HFD_T (n=9)	0.32±0.06 *	0.51±0.03 *	21.39±0.56 *

Within the same column, asterisk indicates significant difference between groups.
* P<.05.

2.3. Xenograft implantation of tumor cells

To achieve our specific aims, we used immunodeficient nude mice and xenografted human colon cancer HT-29 cells under the skin. Human colon cancer HT-29 cells with luciferase reporter gene were purchased from Caliper Life Sciences, Inc. (Hopkinton, MA, USA). Briefly, human colon cancer HT-29 cells were maintained at 37°C in 5% CO_2 incubator and grown to confluency using 10% FBS, 0.2% (w/v) sodium bicarbonate McCoy-supplemented media.

To produce a mouse xenograft model of CRC, subconfluent cultures of colon cancer HT-29 cells were given fresh medium 24 h before being harvested by a brief treatment with 0.25% trypsin and 0.02% EDTA. Trypsinization was stopped with medium containing 10% FBS, and the cells were washed twice and resuspended in serum-free medium. Only single-cell suspensions with a viability of greater than 90% were used for injections.

2.4. Animals and HFD

Female adult (3–4 weeks old) BALB/C AnN-Foxn1 nude mice (18–21 g) were obtained from the National Laboratory Animal Center (Taipei, Taiwan). Mice were maintained under specific pathogen-free conditions in facilities approved by the National Laboratory Animal Center in accordance with current regulations and standards. During the entire experimental period, mice (n=9 for each group) were fed with either an isocaloric standard diet (SD) or HFD purchased from LabDiet, Inc. (St. Louis, MO, USA). The SD contains 13.5% total energy of diet, while the HFD contains 45% total energy of diet as indicated by the supplier. The major source of saturated fatty acids (SFA), monounsaturated fatty acids (MUFA), and polyunsaturated fatty acids (PUFA) in these diets is from corn oil. The actual amount of fat in SD is around 6.2% (SFA: 1.4%; MUFA: 1.52%; n-3 PUFA: 0.12%; n-6 PUFA: 1.82%). The actual amount of fat in HFD is about 23.6% (SFA: 9%; MUFA: 9.32%; n-3 PUFA: 0.32%; n-6 PUFA: 3.48%). These semisynthetic diets consist of similar amount of fat-soluble vitamins such as vitamin E.

Mice anesthetized with an inhalation of isoflurane were placed in a supine position. The mice were subcutaneously injected with ~1 million human colon cancer HT-29 cells (1×10^6/0.1 ml medium) on the right flank of each BALB/C AnN-Foxn1 nude mouse. A well-localized bleb was a sign of a technically satisfactory injection.

After the inoculation, mice were divided into two subgroups (n=9 for each group). For the HFD-fed group (HFD_Tumor), mice received HFD daily. The tumor control group (SD_Tumor) only received SD every day. However, the negative control group without inoculation of cancer cells only received SD. By study end (fifth week), the mice were euthanized with CO_2 inhalation and sacrificed; tumor tissues were frozen immediately, sectioned and stained with hematoxylin–eosin (H&E) for light microscopic analysis.

2.5. Bioluminescence imaging of colorectal carcinoma

Documentation of bioluminescence imaging (BLI) was performed by using *in vivo* imaging system (IVIS) model 200 (Caliper Life Sciences, Hopkinton, MA, USA). Luciferin (15 mg/ml), the substrate of luciferase, was injected into the tumor-bearing mice peritoneally. Results of BLI were analyzed by accessory software. The intensity of bioluminescence was expressed as p/s/cm^2.

2.6. Histopathological and immunofluorescence staining of tumor tissues

Frozen tumor tissues were cut in 5-μm sections and fixed with 4% paraformaldehyde immediately. Sections were stained with Mayer's H&E. Negative controls did not show staining. In a blinded manner, three hotspots were examined per tumor section (high-power fields ×200) of nine different tumors in each group. Images of tumor sections were acquired on an Olympus BX-51 microscope using the Olympus DP-71 digital camera and imaging system.

For immunofluorescence staining, primary colon cancer tissue were frozen, sectioned and subjected to anti-PCNA, anti-$p21^{CIP1/WAF1}$, anti-Vimentin and anti-COX-2 antibodies. The sectioned tissues probed with anti-PCNA or anti-Vimentin

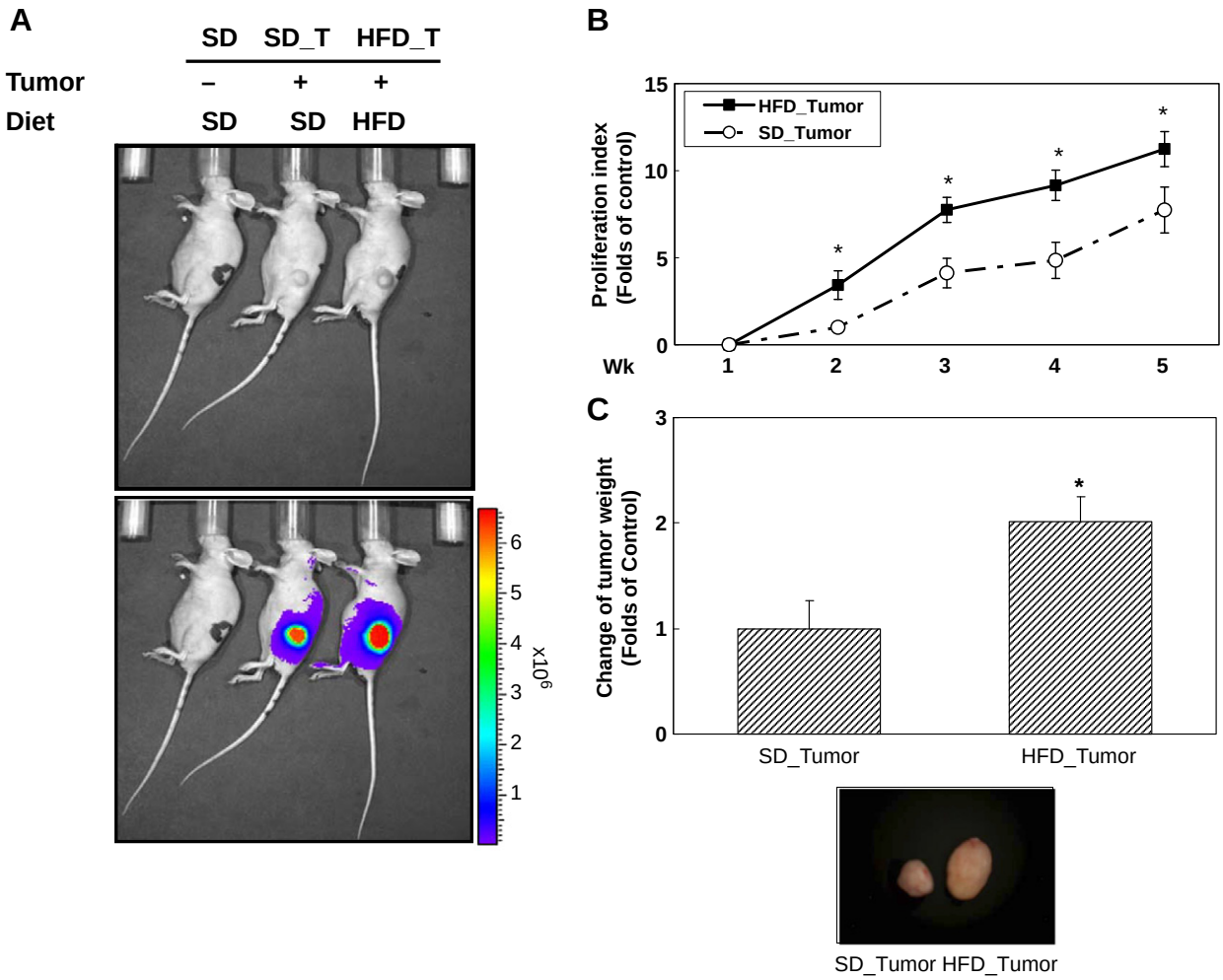

Fig. 1. Consumption of HFD enhanced the growth of colon cancer in a mouse xenograft model. (A) In addition to negative control group (normal group), xenograft nude mice were divided into two groups and given either SD or HFD for 5 weeks (n=9 for each group). The extent of tumor growth was evaluated by using an IVIS 200 BLI system. Luciferin (15 mg/ml), the substrate of luciferase, was injected into the tumor-bearing mice peritoneally. Photos and bioluminescent imaging of primary tumors from each group are shown here. Bioluminescent intensities of tumor tissues represent proliferative levels of CRC at the fifth week. The intensity of bioluminescence was expressed as p/s/cm^2. Proliferative indices were represented by different color scales in descending order (red>orange>yellow>green>light blue>royal blue>purple). The proliferative levels are proportional to the color and area of tumor tissues. SD: SD-fed group without inoculation of cancer cells. SD_Tumor (SD_T): SD-fed group with inoculation of cancer cells. HFD_Tumor (HFD_T): HFD-fed group with inoculation of cancer cells. (B) Xenograft nude mice were given either SD (SD_T) or HFD (HFD_T) for 5 weeks. The BLI of tumor tissues was documented by using an IVIS 200 BLI system and analyzed through Living Image software. Data of bioluminescent intensities represent the real-time proliferation indices of primary tumor tissues. The proliferative index is representative of image intensities compared to the bioluminescence intensity in SD-fed tumor group (SD_T) at week 2. Asterisks represent statistically significant difference compared to the SD-fed group at the same time point, P<.05 (*P<.05). (C) Data represent the change of tumor weight in SD-fed (SD_T) and HFD-fed (HFD_T) groups. Asterisks represent statistically significant difference compared to the SD-fed group (SD_T), P<.05 (*P<.05 at week 5). Documented photos are shown at the bottom panel. (D) Tumor tissues were formalin-fixed, embedded in paraffin, sectioned and subjected to H&E staining. Imaging was documented at 200× magnification. Blue spots represent the nuclei stained with hematoxylin. Red spots represent cytoplasma stained with eosin.

antibody were further subjected to secondary antibody with anti-IgG conjugated fluorescein isothiocyanate (FITC) label. The sectioned tissues probed with anti-p21$^{CIP1/WAF1}$ antibody were further subjected to secondary antibody with rhodamine label. For different experiments, sectioned tissues probed with anti-COX-2 antibody were subjected to either FITC or rhodamine label. Cell nuclei were stained with 4,6-diamidino-2-phenylindole (DAPI). Imaging was documented at 200× magnification. Images of tumor sections were acquired on an Olympus BX-51 microscope using the Olympus DP-71 digital camera and imaging system.

2.7. Western blotting analysis

Nuclear and cytoplasmic fractions from animal tissues were prepared using the Nuclear and Cytoplasmic Extract Reagent Kit containing protease inhibitor and phosphatase inhibitors (Pierce Biotechnology, Rockford, IL, USA). Cross-contamination between nuclear and cytoplasmic fractions was not found (data not shown).

Briefly, tissues were extracted according to the manufacturer's instruction. Cell lysates were cleared by centrifugation. Cellular proteins (100 μg) were fractioned on 10% sodium dodecyl sulfate polyacrylamide gel electrophoresis, transferred to nitrocellulose membrane and blotted with anti-E-cadherin, anti-Twist, anti-Vimentin, anti-N-cadherin, anti-phosphorylation ERK1/2 and anti-phosphorylation mTOR monoclonal antibodies according to the manufacturer's instructions. The blots were stripped and reprobed with β-actin antibody as loading control. Levels of PCNA, cyclin D1, β-catenin, NF-κB p65 (RelA) and $p21^{CIP1/WAF1}$ proteins were measured by using the same procedure described above. The blots were stripped and reprobed with lamin A/C antibody as loading control.

2.8. Analysis of HDACs

The nuclear levels of HDACs in tumor tissues were quantified by HDAC Activity Assay Kit (Cayman Chemical, Ann Arbor, MI, USA). Briefly, 50 μg of nuclear proteins was added to each well and performed according to the manufacturer's instructions. Upon completion of the enzyme-linked immunosorbent assay (ELISA) process, fluorescence intensities were read using an excitation wavelength of 340–360 nm and emission wavelength of 440–465 nm.

2.9. Statistical analysis

The quantitative methodology was used to determine whether differences in the change of tumor weight, proliferation index, biomarker expression levels or HDAC levels exist among SD-fed normal sets (without inoculation of cancer cells), SD-fed tumor groups and HFD-fed tumor groups (n=9 for each group). In brief, statistical analyses of the differences in experimental and control conditions were performed using SYSTAT. Confirmation of differences in HDAC levels as being statistically significant requires rejection of the null hypothesis of no difference among data obtained from experimental and control groups at the P=.05 level with the one-way analysis of variance. The Bonferroni post hoc test was used to determine differences among different groups. Confirmation of differences in other parameters as being statistically significant requires rejection of the null hypothesis of no difference among data obtained from experimental and control groups at the P=.05 level with Student's t test.

3. Results

3.1. Consumption of HFD enhanced the growth of colon cancer in a mouse xenograft model

In the current study, we hypothesized that HFD consumption could enhance tumor growth and progression of colon cancer. To this aim, we used immunodeficient nude mice and xenografted subcutaneously human colon cancer HT-29 cells with luciferase reporter gene into each nude mouse. The composition of experimental diets is listed in Table 1. By study end (fifth week), we measured the total body weight and weights of visceral fat pads and tumor tissues in tumor-bearing nude mice. As shown in Table 2, HFD consumption could significantly increase the total body weight and weights of visceral fat pads and tumor tissues. The tumor weight per mouse significantly increased from 0.15±0.03 g in the SD-fed group (SD_Tumor) to 0.32 ±0.06 g in the HFD-fed group (HFD_Tumor), accounting for 2.13-folds increase in tumor growth (P<.05). Weight of fat pad tissues per mouse significantly increased from 0.31±0.05 g in the SD_Tumor group to 0.51±0.03 g in the HFD_Tumor group, accounting for 1.64-folds increase (P<.05). At the beginning of study, the average body weight was 20.08±0.30 g and 20.33±0.45 g in the SD-fed group and the HFD-fed group, respectively (P=.25). By study end (fifth week), the average body weight significantly increased from 19.52±0.76 g in the SD_Tumor group to 21.39±0.56g in the HFD_Tumor group (P<.05).

We further validated the effects of HFD consumption on tumor growth in a real-time manner by using noninvasive BLI system (Caliper Life Sciences, Inc., Hopkinton, MA, USA). The bioluminescence intensities acquired from imaging represented the proliferation index of colon cancer cells in a mouse xenograft model. To demonstrate the growth rate of colorectal carcinoma in a real-time manner, we measured bioluminescence intensity of each mouse weekly. The initial bioluminescence intensities were still weak and could be confounded by noisy background signals. To obtain accurate data from BLI, bioluminescence intensity at each time point was compared to the initial bioluminescence intensity in the SD_Tumor group at week 2. The adjusted ratio of bioluminescence intensity represented proliferation indices of cancer cells. As shown in Fig. 1A, consumption of HFD significantly augmented the proliferation indices of colon cancer HT-29 cells in tumor-bearing mice. Quantitative analysis of real-time BLI demonstrated that HFD consumption could accelerate tumor growth in a mouse xenograft model (Fig. 1B). In this study, HFD consumption significantly accelerated tumor growth between weeks 2 and 5. At the end of study (fifth week), average BLI intensities increased from 7.74-folds in the SD-fed group to 11.24-folds in the HFD-fed group (P<.05). By study end (fifth week), HFD consumption significantly increased tumor weight up to appropriately 2.13-folds compared to SD (SD_T) in a mouse xenograft model (Fig. 1C). To further identify the effects of HFD on tumor progression, we investigated levels of pathological changes through Mayer's H&E staining of tumor tissues. As shown in Fig. 1D, consumption of HFD increased the levels of proliferating cells in tumor tissues when compared to the SD-fed group (SD_T). These results suggested that HFD consumption could accelerate tumor growth and progression in a mouse xenograft colon cancer model.

3.2. HFD augmented PCNA and COX-2 expression in tumor-bearing mice

As we described above, HFD enhanced tumor growth and progression in tumor-bearing mice. We further investigated whether HFD could modulate the expression of proliferation biomarker (PCNA) and inflammatory biomarker (COX-2) in tumor tissues. Immunofluorescent staining results demonstrated that consumption of HFD could significantly induce the expression of PCNA and COX-2 proteins in tumor tissues (Fig. 2A–B). The results suggested that HFD consumption could induce the tumor growth and inflammation of CRC in tumor-bearing mice. To further investigate the probable mechanism of actions, we examined the effects of HFD on nuclear expression of PCNA, cyclin D1, β-catenin and NF-κB p65 (Rel A) proteins in tumor tissues. As shown in Fig. 2C–D, consumption of HFD could significantly increase nuclear levels of cell cycle modulator proteins such as PCNA and cyclin D1 in tumor tissues. HFD could further increase nuclear levels of transcription factor β-catenin and NF-κB p65 (Rel A) proteins. These results demonstrated that consumption of HFD could mediate the expression of cyclin D1 and COX-2 proteins, which were correlated with the tumor growth and progression of CRC in tumor-bearing mice (Fig. 2). The molecular mechanisms were through the up-regulation of β-catenin and NF-κB p65 (Rel A) proteins, respectively.

3.3. HFD consumption modulated the HDAC levels and suppressed nuclear $p21^{CIP1/WAF1}$ expression in tumor tissues

A previous study indicated that cell cycle inhibitor $p21^{CIP1/WAF1}$ protein could suppress cell proliferation through suppression of PCNA protein. As we described above, HFD could augment PCNA expression in tumor tissues. Therefore, we further investigated whether HFD could modulate $p21^{CIP1/WAF1}$ expression in tumor-bearing mice. Compared to the SD-fed group, consumption of HFD could significantly suppress the nuclear levels of $p21^{CIP1/WAF1}$ protein by up to 90% inhibition in tumor tissues (Fig. 3A). Immunofluorescent staining results also demonstrated that HFD could block the expression of $p21^{CIP1/WAF1}$ protein in tumor tissues (Fig. 3B). Studies indicated that nuclear HDAC levels are correlated with expression of $p21^{CIP1/WAF1}$.

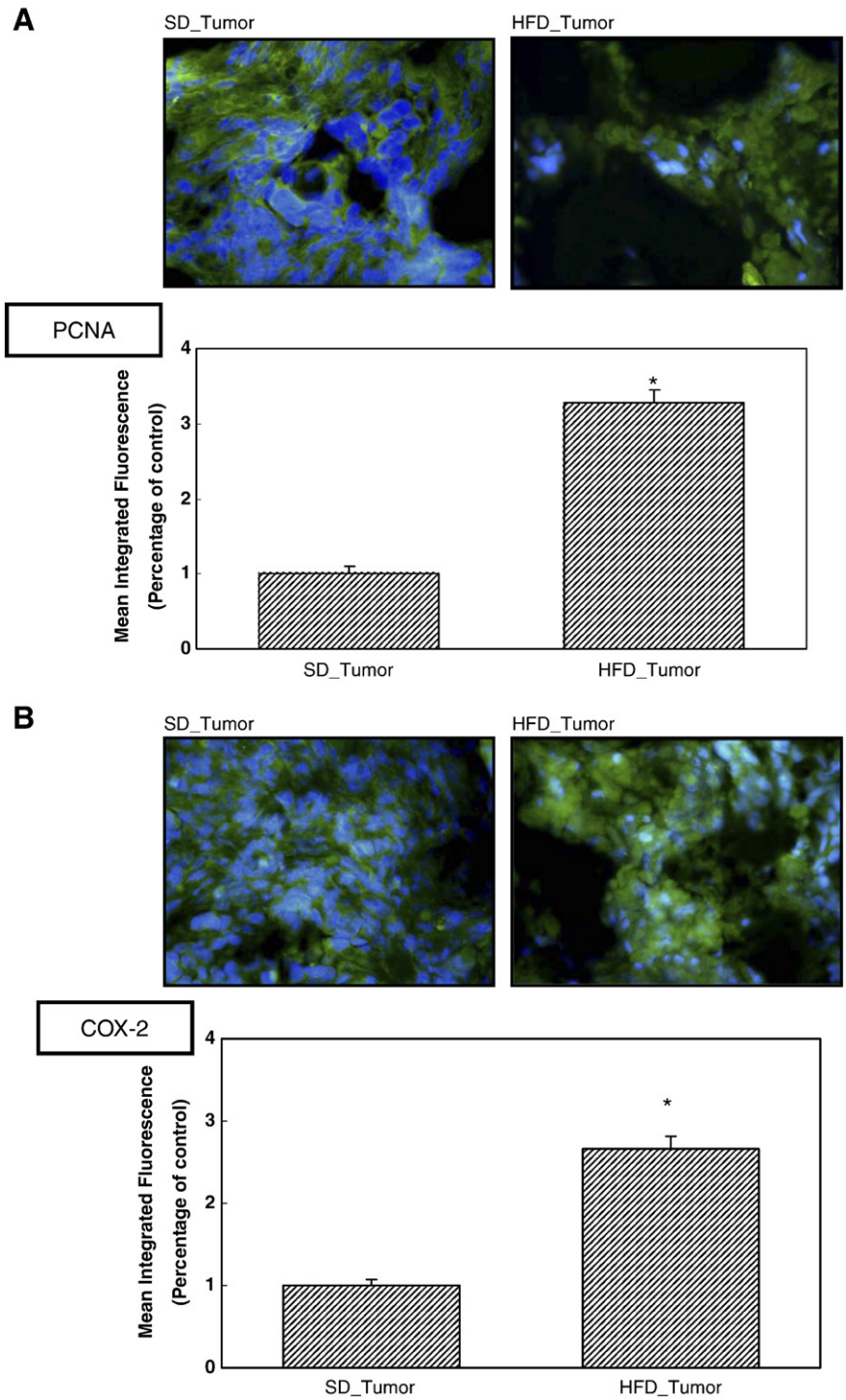

Fig. 2. HFD augmented PCNA and COX-2 expression in tumor-bearing mice. (A) Tumor tissues were frozen, sectioned and subjected to anti-PCNA antibody by immunofluorescence staining described under the Materials and methods section. Imaging was documented at 200× magnification. Green fluorescence area represents distribution of PCNA protein in colon cancer cells stained with monoclonal antibody. Blue fluorescence area represents the location of cell nuclei stained with DAPI. These results presented are representative of nine different experiments. The mean integrated fluorescence of PCNA protein was shown in the bottom panel. Mean integrated fluorescence of HFD-fed tumor group (HFD_T) was compared to the SD-fed tumor control group (SD_T). Asterisk represents statistically significant difference, $P<.05$. (B) Tumor tissues were frozen, sectioned and subjected to anti-COX-2 antibody by immunofluorescence staining described in the Materials and methods section. Imaging was documented at 200× magnification. Green fluorescence area represents distribution of COX-2 protein in colon cancer cells stained with monoclonal antibody. Blue fluorescence area represents the location of cell nuclei stained with DAPI. These results presented are representative of nine different experiments. The mean integrated fluorescence of COX-2 protein is shown in the bottom panel. Asterisks represent statistically significantly difference compared to SD-fed tumor group (SD_T), $P<.05$. (C) Nuclear lysates from tumor tissues were prepared by using Nuclear Extract reagent kit containing protease inhibitor and phosphatase inhibitors according to the manufacturer's instruction. After centrifugation for 10 min at 12,000g to separate cytoplasma fractions, the precipitates were retained and dissolved in buffer as a nuclear extract. Cross contamination between nuclear and cytoplasma fractions was not found (data not shown). Cell lysates were blotted with anti-PCNA, anti-cyclin D1, anti-β-catenin and anti-NF-κB p65 (RelA) monoclonal antibodies as described under Materials and Methods. The levels of detection in nuclear lysate represent the amount of nuclear PCNA, cyclin D1, β-catenin and NF-κB p65 (RelA) proteins in tumor tissues. The blots were stripped and reprobed with anti-lamin AC antibody as loading control. The immunoreactive bands are noted with arrows. (D) The integrated densities of PCNA, cyclin D1, β-catenin and NF-κB p65 (RelA) proteins adjusted with internal control protein (lamin A/C) were shown here. Asterisks represent statistically significantly difference compared to SD-fed tumor group (SD_T), $P<.05$.

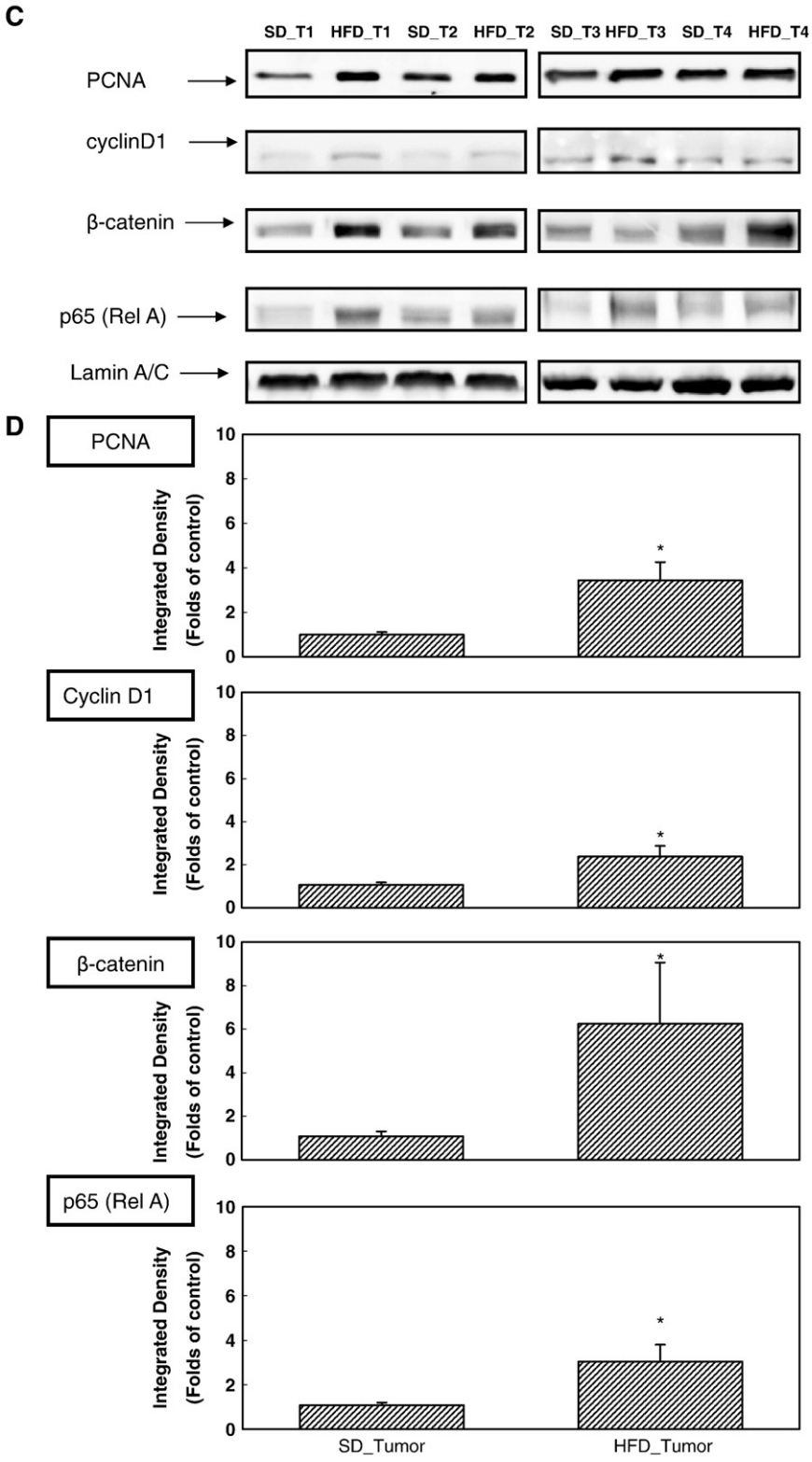

Fig. 2 (*continued*)

HDAC could deacetylate the promoter region of $p21^{CIP1/WAF1}$ gene and suppress gene expression. Therefore, we further examined the effects of HFD consumption on the nuclear levels of HDAC. The results demonstrated that consumption of HFD could augment nuclear HDAC levels by up to almost twofold compared to the nuclear levels of HDAC in SD-fed tumor-bearing mice (Fig. 3C). The dysfunction of tumor suppressor genes such as $p21^{CIP1/WAF1}$ could be associated with HFD-mediated augmentation of HDAC levels in tumor tissues. These novel findings provided supporting evidence for HFD-mediated increases in HDAC levels and epigenetic regulation of $p21^{CIP1/WAF1}$ in CRC.

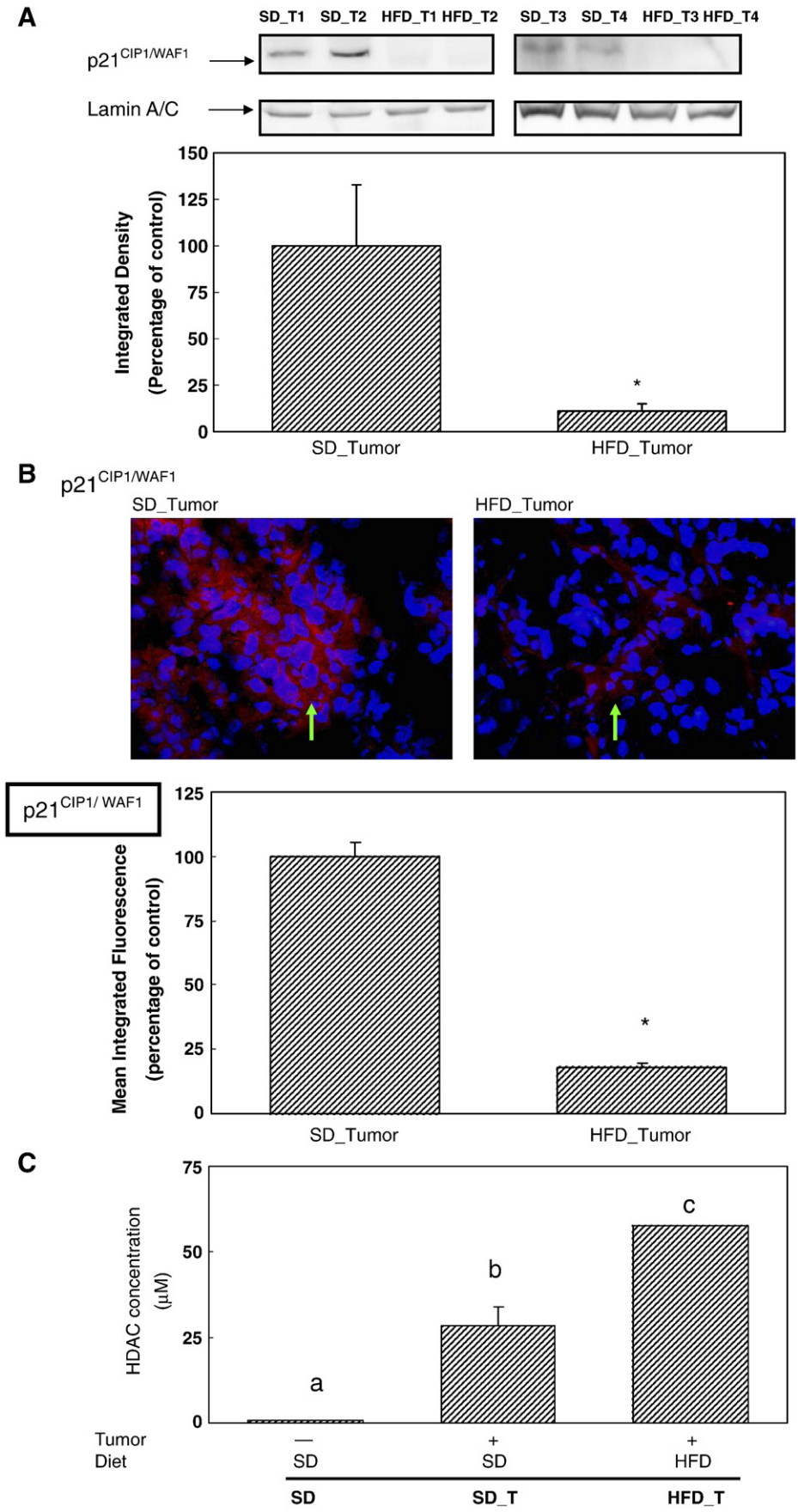
A
SD_T1 SD_T2 HFD_T1 HFD_T2 SD_T3 SD_T4 HFD_T3 HFD_T4
p21CIP1/WAF1
Lamin A/C
Integrated Density (Percentage of control)
150
125
100
75
50
25
0
*
SD_Tumor
HFD_Tumor
B
p21CIP1/WAF1
SD_Tumor
HFD_Tumor
p21CIP1/ WAF1
Mean Integrated Fluorescence (percentage of control)
125
100
75
50
25
0
*
SD_Tumor
HFD_Tumor
C
HDAC concentration (μM)
75
50
25
0
a
b
c
Tumor
Diet
—
SD
+
SD
+
HFD
SD
SD_T
HFD_T

3.4. HFD-mediated loss of E-cadherin proteins was concomitant with activation of ERK1/2 signaling pathway

To understand the probable mechanisms, we further examined the effect of HFD consumption on multiple signaling pathways such as PI3K/Akt/mTOR and MAPK/ERK cascades in tumor-bearing mice. As shown in Fig. 4A, HFD consumption could significantly increase phosphorylation levels of ERK1 and mTOR proteins in tumor tissues. In addition, HFD consumption could also effectively modulate ERK2 activity in tumor-bearing mice. These results suggested that HFD-mediated tumor growth could be associated with activation of MAPK/ERK and PI3K/Akt/mTOR signaling pathways in tumor tissues. Previous studies indicated that functional loss of E-cadherin adherent protein and up-regulation of Twist protein were associated with activation of MAPK/ERK molecules. Therefore, we further investigated the effects of HFD consumption on the expression of E-cadherin and Twist proteins in a mouse xenograft tumor model. As shown in Fig. 4B, the results demonstrated that HFD consumption could mediate the loss of E-cadherin molecule in tumor tissues. Moreover, HFD could augment the expression of Twist protein. Therefore, it is plausible that HFD consumption could aggravate the EMT process through modulation of E-cadherin and Twist proteins in a mouse xenograft colon cancer model.

3.5. Consumption of HFD augmented EMT progression in a mouse xenograft tumor model

To further validate the effects of HFD on EMT progression, we further examined the expression of other EMT biomarker proteins such as Vimentin and N-cadherin proteins in tumor-bearing mice. As shown in Fig. 5A–B, HFD consumption augmented the expression of Vimentin and N-cadherin proteins in tumor tissues. Our novel findings suggested that HFD consumption could accelerate EMT progression through modulation of EMT-related proteins in a mouse xenograft colon cancer model. Collectively, HFD consumption could activate PI3K/Akt/NF-κB and MAPK/ERK signaling cascades to modulate inflammation and EMT progression in a mouse xenograft model. To further validate whether HFD could concomitantly modulate EMT and tumor inflammation, we further investigated the correlation between EMT and tumor inflammation biomarkers in tumor tissues. To this aim, we characterized the colocalization of EMT biomarker (Vimentin) and tumor inflammation biomarker (COX-2) *in situ*. In comparison to the SD-fed tumor-bearing mice, HFD consumption could augment the expression of Vimentin and COX-2 proteins in tumor tissues. Furthermore, intensive colocalization of both Vimentin and COX-2 proteins was found in the HFD-fed tumor group (merged image in Fig. 5C). The results provided novel evidence and suggested that HFD consumption might augment tumor progression including EMT and tumor inflammation in a mouse xenograft colon cancer model. (Fig. 5D).

4. Discussion

A diet–cancer question that has become contentious in recent years is HFD and the role it might play in the development of human CRC. Despite nearly several decades of intensive research, the molecular mechanisms of HFD consumption attributing to the development of human CRC are still unclear. In this study, the results demonstrated that consumption of HFD could induce tumor growth, progression including EMT and tumor inflammation of colon cancer in a mouse xenograft model. As shown in Fig. 1, consumption of HFD augmented the tumor growth in tumor-bearing mice. Noninvasive BLI system demonstrated that HFD could significantly accelerate the growth rate of colorectal tumor. Results of Mayer's H&E staining also suggested that HFD increased levels of proliferative cells in tumor tissues (Fig. 1D). These results were consistent with other important findings in previous epidemiologic studies [2]. Immunofluorescence staining results indicated that HFD-mediated tumor growth was associated with increases in PCNA, which has been identified as a proliferative marker (Fig. 2A). The connection between inflammation and tumorigenesis is well established and has received supporting evidence from pharmacological and epidemiologic data. Here, we reported that HFD could augment the expression of COX-2 protein, an inflammatory biomarker, in tumor tissues (Fig. 2B). These results suggest that HFD could mediate tumor growth and progression including tumor inflammation of colon cancer in a mouse xenograft model. To confirm our findings, we further examined the expression of these important malignant biomarkers by using Western blotting analysis. As shown in Fig. 2C, HFD consumption could induce the expression of cyclin D1 and COX-2 proteins in tumor tissues. The molecular actions of HFD consumption were associated with up-regulation of transcription factors such as β-catenin and NF-κB p65 (RelA). These results suggested that HFD-mediated tumor growth could be associated with increased cell cycle progression. A recent study suggested that loss of JNK2 could synergize with HFD to increase intestinal tumor susceptibility [51]. Although we had not examined the effects of HFD consumption on the JNK2 signaling pathway thoroughly, the results suggested an important role of β-catenin in the regulation of cyclin D1 expression during HFD-mediated tumor growth [19]. A study indicated that $p21^{CIP1/WAF1}$ may serve as a cell cycle inhibitor protein and suppress functions of cyclin D1 and PCNA proteins. Epigenetic regulation of $p21^{CIP1/WAF1}$ expression could be modulated through the HDAC activity. Therefore, we further examined the effects of HFD consumption on HDAC levels and $p21^{CIP1/WAF1}$ expression. Surprisingly, the results showed that HFD could block $p21^{CIP1/WAF1}$ expression through modulation of nuclear HDAC levels in tumor tissues (Fig. 3). These results suggested an inverse correlation between HFD-mediated modulation of HDAC activity and expression of $p21^{CIP1/WAF1}$ tumor suppressor gene in tumor-bearing mice. Recent studies indicated that a high-carbohydrate diet (fat/carbohydrate ratio=0.10) could up-regulate the histone acetyltransferase (HAT) activity and regulate the expression

Fig. 3. HFD consumption modulated the HDAC levels and suppressed nuclear $p21^{CIP1/WAF1}$ expression in tumor tissues. (A) Nuclear lysates from animal tissues were prepared by using Nuclear Extract reagent kit containing protease inhibitor and phosphatase inhibitors according to the manufacturer's instruction. After centrifugation for 10 min at 12,000*g* to separate cytoplasmic fractions, the precipitates were retained and dissolved in buffer as a nuclear extract. Cross-contamination between nuclear and cytoplasmic fractions was not found (data not shown). Cell lysates were blotted with anti-$p21^{CIP1/WAF1}$ antibody as described under Materials and methods. The levels of detection in nuclear lysate represent the amount of $p21^{CIP1/WAF1}$ in nuclei of tumor tissues. The blots were stripped and reprobed with anti-lamin AC antibody as loading control. The immunoreactive bands are noted with arrows. The integrated density of $p21^{CIP1/WAF1}$ protein adjusted with internal control protein (lamin A/C) was shown in the bottom panel. Asterisk represents statistically significant difference compared to SD-fed tumor group (SD_T), $P<.05$. (B) Tumor tissues were frozen, sectioned and subjected to anti-$p21^{CIP1/WAF1}$ antibody by immunofluorescence staining described under Materials and methods. Imaging was documented at 200× magnification. Red fluorescence area with green arrows represents distribution of $p21^{CIP1/WAF1}$ protein in tumor tissues stained with monoclonal antibody. Blue fluorescence area represents the location of cell nuclei stained with DAPI. These results presented are representative of nine different experiments. The mean integrated fluorescence of $p21^{CIP1/WAF1}$ protein is shown in the bottom panel. Asterisk represents statistically significant difference compared to SD-fed tumor group (SD_T), $P<.05$. (C) The nuclear levels of HDAC in tumor tissues were quantified by HDAC Activity Assay Kit (Cayman Chemical). Briefly, equal amount of nuclear proteins (50 μg) from each sample was added to each well and reacted with HDAC substrate according to the manufacturer's instructions. Upon completion of the ELISA process, fluorescence intensities were read using an excitation wavelength of 340–360 nm and emission wavelength of 440–465 nm. The unit of HDAC activities is represented as μM. Different letters represent statistically significant difference among different groups, $P<.05$.

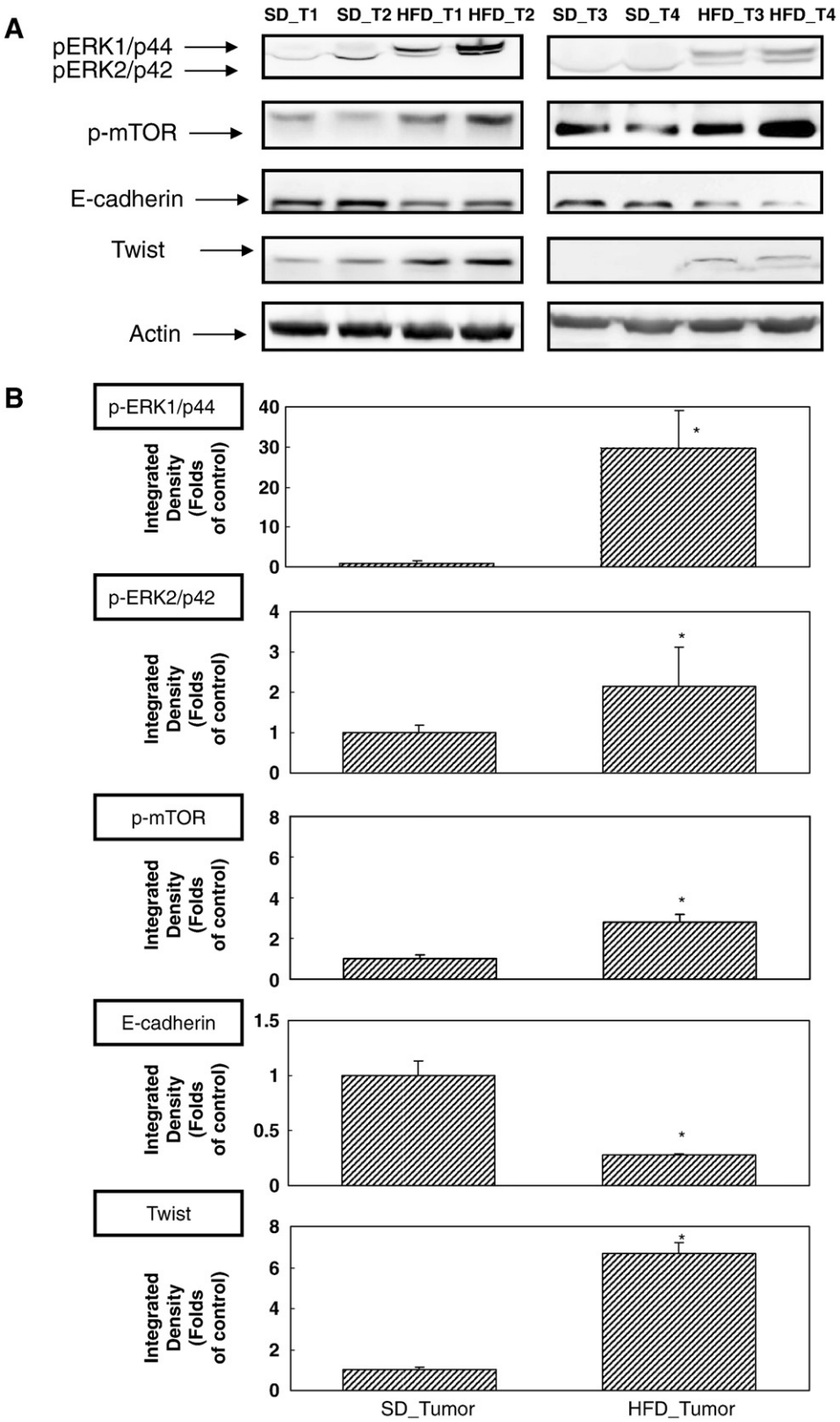

Fig. 4. HFD-mediated loss of E-cadherin proteins was concomitant with activation of ERK1/2 signaling pathway. (A) Cell lysates from animal tissues were prepared using Tissue Extract reagent kit containing protease inhibitor and phosphatase inhibitors according to the manufacturer's instruction. After centrifugation for 10 min at 12,000*g* to remove cell debris, the supernatants were retained as a whole tissue extract. Cross-contamination between nuclear and cytoplasmic fractions was not found (data not shown). Cell lysates were blotted with anti-phosphorylation ERK 1/2, anti-phosphorylation mTOR, anti-E-cadherin and anti-Twist antibodies as described under Materials and methods. The levels of detection in cell lysate represent the amount of phosphorylated ERK 1/2, phosphorylated mTOR, E-cadherin and Twist proteins in cytoplasma of tumor tissues. The blots were stripped and reprobed with anti-actin antibody as loading control. The immunoreactive bands are noted with arrows. (B) The integrated densities of phosphorylated ERK 1/2, phosphorylated mTOR, E-cadherin and Twist proteins adjusted with internal control protein (actin) are shown here. Asterisk represents statistically significant difference compared to the SD-fed tumor group (SD_T), $P<.05$.

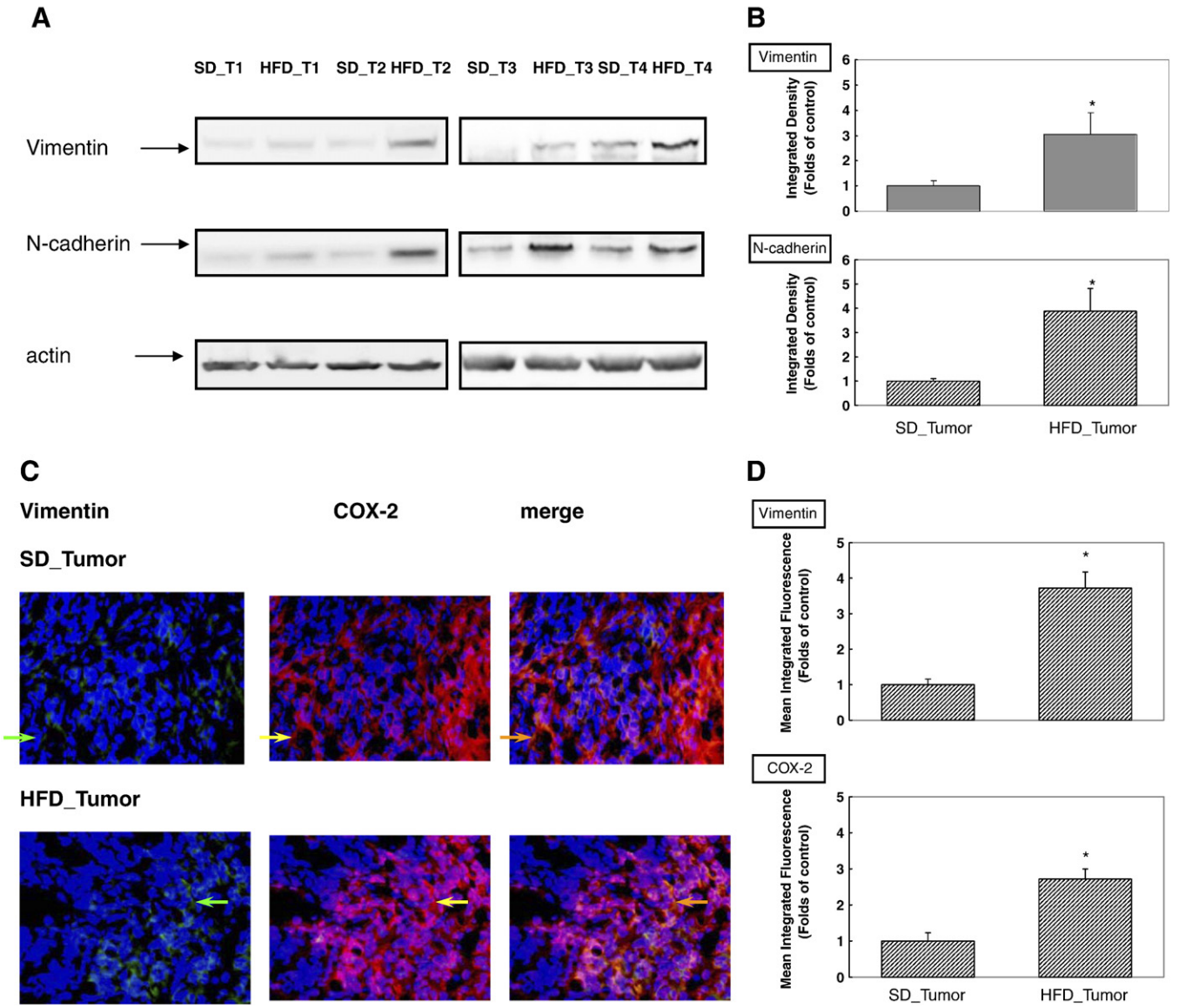

Fig. 5. Consumption of HFD augmented EMT progression in a mouse xenograft tumor model. (A) Cell lysates from animal tissues were prepared using Tissue Extract reagent kit containing protease inhibitor and phosphatase inhibitors according to the manufacturer's instruction. After centrifugation for 10 min at 12,000*g* to remove cell debris, the supernatants were retained as a whole tissue extract. Cross-contamination between nuclear and cytoplasmic fractions was not found (data not shown). Cell lysates were blotted with anti-Vimentin and anti-N-cadherin antibodies as described under Materials and methods. The levels of detection in cell lysate represent the amount of Vimentin and N-cadherin in cytoplasma of tumor tissues. The blots were stripped and reprobed with anti-actin antibody as loading control. The immunoreactive bands are noted with arrows. (B) The integrated densities of Vimentin and N-cadherin proteins adjusted with internal control protein (actin) are shown here. Asterisk represents statistically significant difference compared to SD-fed tumor group (SD_T), $P<.05$. (C) Tumor tissues were frozen, sectioned and subjected to anti-Vimentin and anti-COX-2 antibodies by immunofluorescence staining described under Materials and methods. Imaging was documented at 200× magnification. Green fluorescence area indicated with green arrows represents distribution of Vimentin protein in tumor tissues stained with monoclonal antibody. Red fluorescence area indicated with yellow arrows represents distribution of COX-2 protein in tumor tissues stained with monoclonal antibody. Yellow fluorescence area indicated with orange arrows in merged imaging represents the colocalization of Vimentin and COX-2 proteins in tumor tissues. Blue fluorescence area represents the location of cell nuclei stained with DAPI. These results presented are representative of nine different experiments. (D) The mean integrated fluorescence of Vimentin and COX-2 proteins is shown. Asterisk represents statistically significant difference compared to SD-fed tumor group (SD_T), $P<.05$.

of several genes when compared to the HFD (fat/carbohydrate ratio=14.6) in normal intestinal cells [52]. In the present study, we adapted an HFD model that is similar to Western-style diet. Our results demonstrated that the HFD used in this study (fat/carbohydrate ratio=1.26) could further induce the HDAC activity in tumor tissues. It suggested that HFD could modulate the HDAC and HAT activities in normal and malignant cells [52,53]. It is plausible that HFD could increase the HDAC activity and modulate the expression of $p21^{CIP1/WAF1}$ gene through epigenetic modification of chromosome in tumor-bearing mice. Taken together; our results provide novel evidence to support the epigenetic regulation of tumor suppressor genes, which is mediated by HFD consumption in a mouse xenograft tumor model.

The increased expression of NF-κB p65 (RelA) and COX-2 may result in a significant acceleration of tumor progression in these mice. To validate the importance of these findings, we further investigated the effects of HFD consumption on EMT progression in tumor-bearing mice. As shown in Fig. 4, our results demonstrated that HFD consumption could activate the MAPK/ERK and PI3K/Akt/mTOR signaling pathways of colon cancer in a mouse xenograft tumor model. Consumption of HFD could further modulate the EMT process in tumor tissues. The molecular mechanisms of HFD consumption

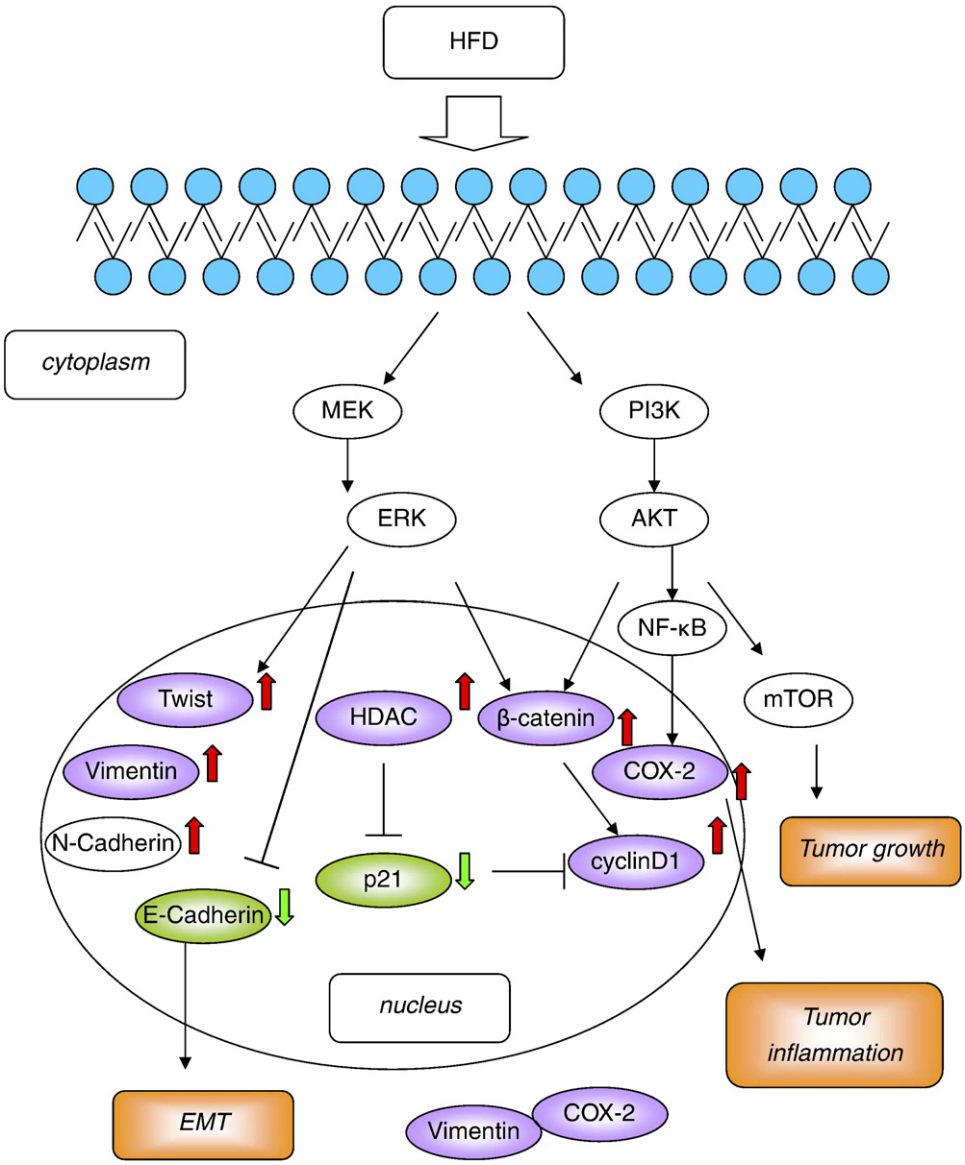

Fig. 6. Proposed mechanisms of signaling pathways associated with HFD-mediated tumor growth and progression including EMT and inflammation. Red arrows indicate increases in expression level. Green arrows indicate decreases in expression level. → : induction; ⊣ : suppression.

were through functional loss of E-cadherin and up-regulation of EMT biomarkers such as Twist, Vimentin and N-cadherin proteins (Figs. 4–5). Moreover, the results demonstrated HFD-mediated colocalization of Vimentin and COX-2 proteins in tumor tissues. It suggested a strong correlation between EMT and tumor inflammation in HFD-fed tumor-bearing mice. Taken together, we propose a model of HFD-mediated tumor growth and progression including EMT and inflammation in tumor-bearing mice (Fig. 6). Here, our results suggest that HFD consumption could modulate HDAC activity and inhibit the expression of $p21^{CIP1/WAF1}$ through epigenetic regulation. Moreover, HFD could activate the PI3K/Akt/mTOR and MAPK/ERK signaling pathways, which drive tumor growth through up-regulation of NF-κB, β-catenin, PCNA and cyclin D1 proteins in tumor tissues. Our data strongly suggest that HFD could concomitantly augment tumor progression including EMT and inflammation of colon cancer in tumor-bearing mice. The molecular mechanisms were through the up-regulation of COX-2, Twist, Vimentin and N-cadherin proteins and functional loss of E-cadherin in tumor-bearing mice. In conclusion, our novel findings demonstrated that HFD consumption could play important roles in tumor growth and progression including EMT and tumor inflammation in a mouse xenograft model.

Acknowledgments

This material is based upon work supported by the National Science Council grant under agreement no. 97-2320-B-039-043-MY3 and the China Medical University grant under agreement no. CMU98-S-26. Any opinions, findings, conclusions or recommendations expressed in this publication are those of the authors and do not necessarily reflect the view of the National Science Council and China Medical University.

References

[1] Jemal A, Siegel R, Xu J, Ward E. Cancer statistics, 2010. CA Cancer J Clin 2010;60: 277–300.

[2] Meyerhardt JA, Niedzwiecki D, Hollis D, Saltz LB, Hu FB, Mayer RJ, et al. Association of dietary patterns with cancer recurrence and survival in patients with stage III colon cancer. JAMA 2007;298:754–64.
[3] Slattery ML, Boucher KM, Caan BJ, Potter JD, Ma KN. Eating patterns and risk of colon cancer. Am J Epidemiol 1998;148:4–16.
[4] Slattery ML, Potter JD, Duncan DM, Berry TD. Dietary fats and colon cancer: assessment of risk associated with specific fatty acids. Int J Cancer 1997;73:670–7.
[5] Larue L, Bellacosa A. Epithelial-mesenchymal transition in development and cancer: role of phosphatidylinositol 3′ kinase/AKT pathways. Oncogene 2005;24:7443–54.
[6] Lipsky PE. Role of cyclooxygenase-1 and -2 in health and disease. Am J Orthop (Belle Mead NJ) 1999;28:8–12.
[7] Loboda A, Nebozhyn MV, Watters JW, Buser CA, Shaw PM, Huang PS, et al. EMT is the dominant program in human colon cancer. BMC Med Genomics 2011;4:9.
[8] Castro-Carpeno J, Belda-Iniesta C, Casado SE, Hernandez AE, Feliu BJ, Gonzalez BM. EGFR and colon cancer: a clinical view. Clin Transl Oncol 2008;10:6–13.
[9] Johnson SM, Gulhati P, Rampy BA, Han Y, Rychahou PG, Doan HQ, et al. Novel expression patterns of PI3K/Akt/mTOR signaling pathway components in colorectal cancer. J Am Coll Surg 2010;210:767–8.
[10] Lu Z, Cox-Hipkin MA, Windsor WT, Boyapati A. 3-Phosphoinositide-dependent protein kinase-1 regulates proliferation and survival of cancer cells with an activated mitogen-activated protein kinase pathway. Mol Cancer Res 2010;8:421–32.
[11] Morgensztern D, McLeod HL. PI3K/Akt/mTOR pathway as a target for cancer therapy. Anticancer Drugs 2005;16:797–803.
[12] Petroulakis E, Mamane Y, Le Bacquer O, Shahbazian D, Sonenberg N. mTOR signaling: implications for cancer and anticancer therapy. Br J Cancer 2006;94:195–9.
[13] Raufman JP, Shant J, Guo CY, Roy S, Cheng K. Deoxycholyltaurine rescues human colon cancer cells from apoptosis by activating EGFR-dependent PI3K/Akt signaling. J Cell Physiol 2008;215:538–49.
[14] Baldassarre G, Nicoloso MS, Schiappacassi M, Chimienti E, Belletti B. Linking inflammation to cell cycle progression. Curr Pharm Des 2004;10:1653–66.
[15] Prescott SM, Fitzpatrick FA. Cyclooxygenase-2 and carcinogenesis. Biochim Biophys Acta 2000;1470:M69–78.
[16] McCubrey JA, Steelman LS, Chappell WH, Abrams SL, Wong EW, Chang F, et al. Roles of the Raf/MEK/ERK pathway in cell growth, malignant transformation and drug resistance. Biochim Biophys Acta 2007;1773:1263–84.
[17] Arber N, Doki Y, Han EK, Sgambato A, Zhou P, Kim NH, et al. Antisense to cyclin D1 inhibits the growth and tumorigenicity of human colon cancer cells. Cancer Res 1997;57:1569–74.
[18] Qiao L, Shiff SJ, Rigas B. Sulindac sulfide inhibits the proliferation of colon cancer cells: diminished expression of the proliferation markers PCNA and Ki-67. Cancer Lett 1997;115:229–34.
[19] Tetsu O, McCormick F. Beta-catenin regulates expression of cyclin D1 in colon carcinoma cells. Nature 1999;398:422–6.
[20] Zhao JH, Luo Y, Jiang YG, He DL, Wu CT. Knockdown of beta-catenin through shRNA cause a reversal of EMT and metastatic phenotypes induced by HIF-1alpha. Cancer Invest 2011;29(6):377–82.
[21] Kanwar SS, Yu Y, Nautiyal J, Patel BB, Majumdar AP. The Wnt/beta-catenin pathway regulates growth and maintenance of colonospheres. Mol Cancer 2010;9:212.
[22] Agarwal C, Singh RP, Dhanalakshmi S, Tyagi AK, Tecklenburg M, Sclafani RA, et al. Silibinin upregulates the expression of cyclin-dependent kinase inhibitors and causes cell cycle arrest and apoptosis in human colon carcinoma HT-29 cells. Oncogene 2003;22:8271–82.
[23] Cayrol C, Knibiehler M, Ducommun B. p21 binding to PCNA causes G1 and G2 cell cycle arrest in p53-deficient cells. Oncogene 1998;16:311–20.
[24] Wilson AJ, Byun DS, Nasser S, Murray LB, Ayyanar K, Arango D, et al. HDAC4 promotes growth of colon cancer cells via repression of p21. Mol Biol Cell 2008;19:4062–75.
[25] Hitomi T, Matsuzaki Y, Yokota T, Takaoka Y, Sakai T. p15(INK4b) in HDAC inhibitor-induced growth arrest. FEBS Lett 2003;554:347–50.
[26] Zupkovitz G, Grausenburger R, Brunmeir R, Senese S, Tischler J, Jurkin J, et al. The cyclin-dependent kinase inhibitor p21 is a crucial target for histone deacetylase 1 as a regulator of cellular proliferation. Mol Cell Biol 2010;30:1171–81.
[27] Wendt MK, Taylor MA, Schiemann BJ, Schiemann WP. Downregulation of epithelial cadherin is required to initiate metastatic outgrowth of breast cancer. Mol Biol Cell 2011;22:2423–35.
[28] Serova M, Astorgues-Xerri L, Bieche I, Albert S, Vidaud M, Benhadji KA, et al. Epithelial-to-mesenchymal transition and oncogenic Ras expression in resistance to the protein kinase Cbeta inhibitor enzastaurin in colon cancer cells. Mol Cancer Ther 2010;9:1308–17.
[29] Mandal M, Myers JN, Lippman SM, Johnson FM, Williams MD, Rayala S, et al. Epithelial to mesenchymal transition in head and neck squamous carcinoma: association of Src activation with E-cadherin down-regulation, vimentin expression, and aggressive tumor features. Cancer 2008;112:2088–100.
[30] Bracke ME, Van Roy FM, Mareel MM. The E-cadherin/catenin complex in invasion and metastasis. Curr Top Microbiol Immunol 1996;213:123–61.
[31] Birchmeier W, Behrens J. Cadherin expression in carcinomas: role in the formation of cell junctions and the prevention of invasiveness. Biochim Biophys Acta 1994;1198:11–26.
[32] Maier HJ, Schmidt-Strassburger U, Huber MA, Wiedemann EM, Beug H, Wirth T. NF-kappaB promotes epithelial-mesenchymal transition, migration and invasion of pancreatic carcinoma cells. Cancer Lett 2010;295:214–28.
[33] van Zijl F, Zulehner G, Petz M, Schneller D, Kornauth C, Hau M, et al. Epithelial-mesenchymal transition in hepatocellular carcinoma. Future Oncol 2009;5:1169–79.
[34] Cai Z, Wang Q, Zhou Y, Zheng L, Chiu JF, He QY. Epidermal growth factor-induced epithelial-mesenchymal transition in human esophageal carcinoma cells–a model for the study of metastasis. Cancer Lett 2010;296:88–95.
[35] Bates RC. Colorectal cancer progression: integrin alphavbeta6 and the epithelial-mesenchymal transition (EMT). Cell Cycle 2005;4:1350–2.
[36] Spaderna S, Schmalhofer O, Hlubek F, Berx G, Eger A, Merkel S, et al. A transient, EMT-linked loss of basement membranes indicates metastasis and poor survival in colorectal cancer. Gastroenterology 2006;131:830–40.
[37] Jung JW, Hwang SY, Hwang JS, Oh ES, Park S, Han IO. Ionising radiation induces changes associated with epithelial-mesenchymal transdifferentiation and increased cell motility of A549 lung epithelial cells. Eur J Cancer 2007;43:1214–24.
[38] Schneider MR, Dahlhoff M, Horst D, Hirschi B, Trulzsch K, Muller-Hocker J, et al. A key role for E-cadherin in intestinal homeostasis and Paneth cell maturation. PLoS One 2010;5:e14325.
[39] Satelli A, Li S. Vimentin in cancer and its potential as a molecular target for cancer therapy. Cell Mol Life Sci 2011;68:3033–46.
[40] Zhang W, Wang J, Zou B, Sardet C, Li J, Lam CS, et al. Four and a half LIM protein 2 (FHL2) negatively regulates the transcription of E-cadherin through interaction with Snail1. Eur J Cancer 2011;47:121–30.
[41] Joyce T, Cantarella D, Isella C, Medico E, Pintzas A. A molecular signature for epithelial to mesenchymal transition in a human colon cancer cell system is revealed by large-scale microarray analysis. Clin Exp Metastasis 2009;26:569–87.
[42] Roger L, Jullien L, Gire V, Roux P. Gain of oncogenic function of p53 mutants regulates E-cadherin expression uncoupled from cell invasion in colon cancer cells. J Cell Sci 2010;123:1295–305.
[43] Jang TJ, Jeon KH, Jung KH. Cyclooxygenase-2 expression is related to the epithelial-to-mesenchymal transition in human colon cancers. Yonsei Med J 2009;50:818–24.
[44] Honma N, Genda T, Matsuda Y, Yamagiwa S, Takamura M, Ichida T, et al. MEK/ERK signaling is a critical mediator for integrin-induced cell scattering in highly metastatic hepatocellular carcinoma cells. Lab Invest 2006;86:687–96.
[45] Ray RM, Vaidya RJ, Johnson LR. MEK/ERK regulates adherens junctions and migration through Rac1. Cell Motil Cytoskeleton 2007;64:143–56.
[46] Tang FY, Chiang EP, Chung JG, Lee HZ, Hsu CY. S-allylcysteine modulates the expression of E-cadherin and inhibits the malignant progression of human oral cancer. J Nutr Biochem 2009;20:1013–20.
[47] Neal CL, McKeithen D, Odero-Marah VA. Snail negatively regulates cell adhesion to extracellular matrix and integrin expression via the MAPK pathway in prostate cancer cells. Cell Adh Migr 2011:5.
[48] Chen X, Halberg RB, Burch RP, Dove WF. Intestinal adenomagenesis involves core molecular signatures of the epithelial-mesenchymal transition. J Mol Histol 2008;39:283–94.
[49] Hong KO, Kim JH, Hong JS, Yoon HJ, Lee JI, Hong SP, et al. Inhibition of Akt activity induces the mesenchymal-to-epithelial reverting transition with restoring E-cadherin expression in KB and KOSCC-25B oral squamous cell carcinoma cells. J Exp Clin Cancer Res 2009;28:28.
[50] Khasawneh J, Schulz MD, Walch A, Rozman J, Hrabed A, Klingenspor M, et al. Inflammation and mitochondrial fatty acid beta-oxidation link obesity to early tumor promotion. Proc Natl Acad Sci U S A 2009;106:3354–9.
[51] Bi X, Pohl NM, Yin Z, Yang W. Loss of JNK2 increases intestinal tumor susceptibility in Apc1638+/− mice with dietary modulation. Carcinogenesis 2011;32:584–8.
[52] Honma K, Mochizuki K, Goda T. Inductions of histone H3 acetylation at lysine 9 on SGLT1 gene and its expression by feeding mice a high carbohydrate/fat ratio diet. Nutrition 2009;25:40–4.
[53] Yorita S, Mochizuki K, Goda T. Induction of histone acetylation on the sucrase-isomaltase gene in the postnatal rat jejunum. Biosci Biotechnol Biochem 2009;73:933–5.